

MoSA: Mixture of Sparse Adapters for Visual Efficient Tuning

Qizhe Zhang¹, Bocheng Zou², Ruichuan An³, Jiaming Liu¹, and Shanghang Zhang¹

¹ National Key Laboratory for Multimedia Information Processing,
School of Computer Science, Peking University
{theia, jiamingliu, shanghang}@pku.edu.cn

² University of Wisconsin-Madison
{bochengz}@cs.wisc.edu

³ School of Software Engineering, Xi'an Jiaotong University
{arctanx}@stu.xjtu.edu.cn

Abstract. With the rapid growth in the scale of pre-trained foundation models, parameter-efficient fine-tuning techniques have gained significant attention, among which Adapter Tuning is the most widely used. Despite achieving efficiency, it still underperforms full fine-tuning, and the performance improves at the cost of an increase in parameters. Recent efforts have either focused on training multiple adapter experts to increase model capacity or on pruning adapters to achieve parameter efficiency. However, both approaches introduce more parameters compared to the original adapter, hence are not computationally efficient. Motivated by this, we propose **Mixture of Sparse Adapters**, or **MoSA**, as a novel Adapter Tuning method to fully unleash the potential of each parameter in the adapter. We first split the standard adapter into multiple non-overlapping modules, then stochastically activate them for sparse training, and finally merge them to form a complete adapter after tuning. In this way, MoSA can achieve significantly better performance than standard adapters without any additional computational or storage overhead. Furthermore, we propose a hierarchical sparse strategy to better leverage limited training data. Extensive experiments on a series of 27 visual tasks demonstrate that MoSA consistently outperforms other Adapter Tuning methods as well as other baselines by a large margin. Furthermore, MoSA brings consistent improvements across various model scales, architectures, and different PEFT methods. Code will be released.

Keywords: Adapter Tuning · Mixture-of-Experts · Sparse Training

1 Introduction

The *pretrain-then-finetune* paradigm has achieved remarkable success in deep learning. Within the field of computer vision, models pre-trained on large-scale datasets (*e.g.* ImageNet-21k [66], JFT-300M [68], SA-1B [40]) have demonstrated significant performance improvements across various downstream tasks [9, 28, 29]. After pre-training, models require fine-tuning on specific data to transfer learned

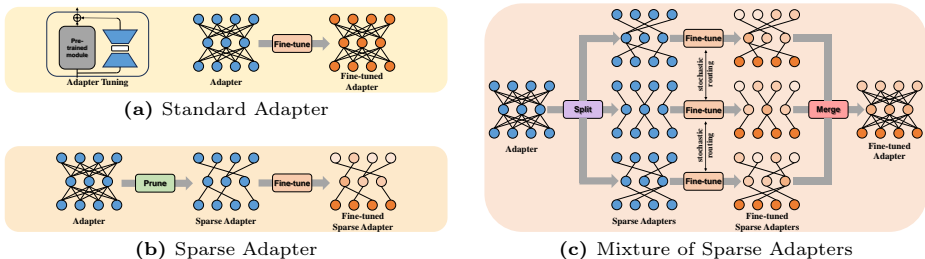


Fig. 1: Different Adapter Tuning diagrams: (a) The standard adapter simply inserts a bottleneck module into each Transformer layer. (b) Sparse Adapter. It prunes the standard adapter before tuning, updating only a small subset of the retained parameters. (c) Our proposed Mixture of Sparse Adapters (MoSA). We first split the standard adapter into multiple non-overlapping modules, then stochastically activate them for sparse training, and finally merge them to form a complete dense adapter.

knowledge to the target domain. The most direct method is *full fine-tuning*, involving the update of all parameters in the pre-trained model during tuning. However, as the scale of pre-trained models continues to grow (*e.g.* ViT-G/14 [81] 1.8B, LVM [2] 3B), storing a complete copy of all parameters for each task becomes impractical, giving rise to a more efficient method of tuning, known as *parameter-efficient fine-tuning* (PEFT). For each downstream task, PEFT updates only a small portion of the parameters in the pre-trained model, achieving efficiency in parameter storage and data utilization.

Recently, various PEFT methods have emerged [31, 34, 36, 39, 45–49, 80, 85], with one of the most widely used being *Adapter Tuning* [7, 8, 33, 60, 61, 64, 65]. This kind of method introduces lightweight bottleneck modules to the pre-trained model while freezing the backbone, as shown in Figure 1(a), facilitating efficient knowledge transfer to downstream tasks. Despite the respectable performance of these methods, they still fall behind full fine-tuning in many scenarios [25] (*e.g.* training data is relatively abundant, the distribution gap between the downstream and pre-training data is significant). Simply increasing the bottleneck dimension can raise performance, but this contradicts the original design philosophy of Adapter Tuning. Recent work has enhanced adapter performance by incorporating a Mixture-of-Experts (MoE) mechanism [16, 18, 21, 79], but having multiple parallel adapter modules and routers introduces additional parameters and computation. Sparsely or stochastically activated MoE is more efficient in implementation [6, 18, 73], but this reduces the amount of data seen by individual experts, an issue we call *data dilution*, leading to even worse performance, especially when training data is limited. Meanwhile, another way for improving adapters involves pruning before tuning [30] (*e.g.* a $4\times$ larger adapter with a 75% sparse ratio), as in Figure 1(b), which has shown performance gains but does not offer computational efficiency, and high levels of sparsity can further lead to training instability. The delicate balance between parameter efficiency and performance remains a key challenge in Adapter Tuning.

Therefore, a natural question arises: **is it possible to achieve both efficiency and performance simultaneously?** In this paper, we propose **Mixture of Sparse Adapters (MoSA)** as an affirmative answer to this question, enhancing adapter performance without introducing additional computational and storage overhead, which is shown in Figure 1(c). We start by splitting the standard adapter into several non-overlapping modules, each can be considered as a sparse expert. During training, to avoid extra computational costs, we use a non-routing stochastic activation mechanism. Each activated module uses a mask to filter gradients, achieving sparsity in parameter updates. We merge all sparse adapters into a complete dense adapter, achieving efficiency in both storage and computation during inference. Through this design, the potential of the original adapter is fully unleashed, maximizing the elimination of parameter redundancy.

Rather than simply stacking two independent approaches, our design organically integrates the stochastically activated MoE with sparse training, where the two components mutually reinforce each other. On one hand, sparse update of parameters more efficiently utilizes training data, alleviating the data dilution caused by sparse activation of multiple experts. On the other hand, the training process with mixed experts ensures expressive capability and stability in downstream tasks, addressing the limitations of sparse training. To better facilitate the combination of the two components, we further propose a hierarchical sparse strategy. The dense down-projection layer provides robust intermediate features for the model, while multiple sparse up-projection layers increase the capacity of the model. It’s worth noting that our approach, as a *general concept* of enhancing parameter utilization, can be applied to various adapter structures and other addition-based PEFT methods. On 27 diverse downstream visual tasks, our MoSA consistently outperforms all other fine-tuning methods, including full fine-tuning. Compared to full fine-tuning, MoSA achieves a lead of 1.36% (on FGVC), 2.43% (on VTAB) and 1.51% (on GICD), while updating only around 1% of the backbone parameters. Compared to the standard adapter, MoSA achieves an improvement of 1.32% (on FGVC) and 1.06% (on VTAB) without adding any computational or storage overhead. Additionally, we conducted comprehensive ablation experiments to validate the effectiveness of each component in our design. The results demonstrate that MoSA is indeed an Adapter Tuning method that successfully balances efficiency and performance.

We summarize our main contributions as follows:

- We propose a novel Adapter Tuning method, namely **MoSA**, for fully unleashing the potential of the standard adapters. Through a mixed and sparse training approach involving splitting and merging, our method maximizes parameter efficiency, enhancing the performance of adapters in visual tasks.
- MoSA best achieves a balance between efficiency and performance. It exhibits efficiency in all the sparsification, mixed training, and inference stages, and the mutual promotion between stochastic activation and sparse training further enhances performance.

- We evaluate our method on a total of 27 downstream visual tasks spanning different domains, and MoSA significantly outperforms full fine-tuning as well as all other PEFT baselines, demonstrating the rationality of our design.
- We conduct comprehensive ablation studies to explore various design choices, demonstrating the effectiveness of each component. Additionally, we showcase the consistent improvements brought by MoSA across multiple model scales, architectures, and different PEFT methods.

2 Related Work

Parameter-efficient fine-tuning (PEFT). Recently, many large-scale pre-trained models (*e.g.* LLaMA2 [69] 70B, GPT-3 [5] 175B) have emerged in deep learning research, which can achieve excellent performance in a variety of downstream tasks. However, updating and storing all model parameters for each task has become far more expensive. PEFT achieves efficiency in training and storage by updating only a small fraction of parameters compared to pre-trained models [27, 36, 37, 45–48, 50, 80, 85], among which Adapter Tuning [8, 33, 60, 61, 64, 65] is one of the most widely used. Due to space constraints, we focus exclusively on Adapter Tuning. For a broader overview of other PEFT methods, we recommend readers refer to surveys on tuning [14, 76]. Adapters [33, 64] are first introduced in natural language processing (NLP), achieving efficient knowledge transfer by only updating the parameters of newly added lightweight bottleneck modules. AdaptFormer [7] first applies adapters to visual recognition, achieving remarkable results in video understanding. Subsequent works [31, 34, 39] implement low-rank adaptation through various decomposition manners, further reducing the number of parameters required for fine-tuning. MoA [44] addresses the domain generalization through a MoE version of the aforementioned adaptation methods. Recently, SparseAdapter [30] enhances parameter efficiency through pruning of adapters before tuning. Although both MoE and sparsification can improve adapter performance, they also introduce additional computational costs. In this work, we propose a novel Adapter Tuning framework that enables two techniques to mutually enhance each other, ensuring both efficiency and performance.

Mixture-of-Experts (MoE). The origin proposal of MoE [35] is targeted at enhancing model capacity. The earliest proposed technologies, known as soft MoE [55], integrate outputs of multiple experts through weighted summation. However, this technique significantly increases the computational cost during training. To address this issue, the sparsely-gated MoE [27, 67, 84] was introduced, selecting specific experts for activation and directly assigning data to them, thereby reducing the computational burden. Nonetheless, this method often resulted in load imbalance, with some experts becoming inactive in later training stages, risking system collapse. THOR [86] effectively mitigates this issue by implementing random activation, which not only enhances efficiency but also improves overall model performance. AdaMix [73] extends this mechanism to efficient tuning, treating each PEFT module as an expert and achieving performance improvements in NLP tasks. However, the stochastic activation of

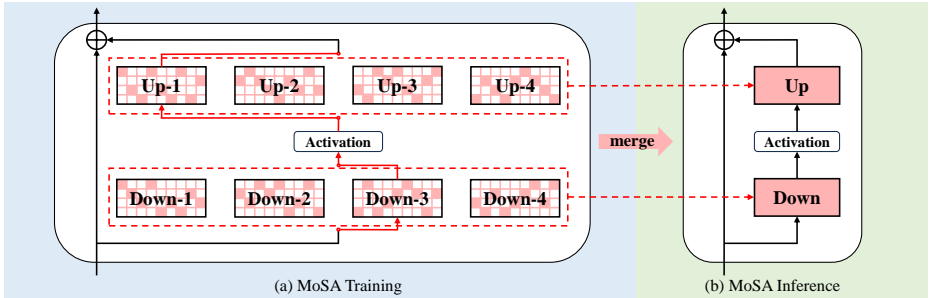


Fig. 2: Architecture design of Mixture of Sparse Adapters. In the training phase, MoSA stochastically activates a sparse adapter during each forward pass; in the inference phase, MoSA merges multiple sparse adapters into a complete one to enhance efficiency.

multiple experts may lead to the issue of data dilution issue, resulting in sub-optimal performance when there is insufficient data for downstream tasks. To address this problem, we employ sparse training for each expert, reducing the data requirement per expert. This approach significantly enhances performance while maintaining the same computational efficiency as standard adapters.

Pruning and sparse training. The primary goal of model pruning [26, 54, 58] aims to minimize deployment costs by reducing model parameters without significantly impacting its performance. Recent studies [1, 24, 75] have revealed that pruning can enhance model fine-tuning. A reduced number of trainable parameters can act as an additional regularization constraint, potentially improving performance [85]. As a PEFT method, the architecture of adapters [33, 64] inherently possesses few updatable parameters. SparseAdapter [1] extends this concept by pre-pruning the adapter, enhancing parameter efficiency while maintaining or even improving performance compared to standard adapters. However, excessive sparsity can lead to training instability and suboptimal results on certain datasets. We take one step further to solve aforementioned weakness via integrating the MoE paradigm into our sparse tuning process. This integration not only achieves a sparse network structure, but also implements sparse activation during the training phase, which overcomes the inherent constraints of using a single sparse network and increases the model capacity.

3 Method

To achieve the optimal balance between efficiency and performance, we propose Mixture of Sparse Adapters (MoSA). The overall design of our method is shown in Figure 2. We first overview our method in Section 3.1. Subsequently, we describe how we split the standard adapter into multiple sparse adapters in Section 3.2. Then, we introduce the training strategy with stochastic activation of multiple sparse experts in Section 3.3. Finally, we merge the split sparse adapters into a complete one for efficiency during inference in Section 3.4.

3.1 Overview

Adapter Tuning is commonly employed in Transformer-based networks, which adapts the pre-trained representation to the target domain by injecting bottleneck modules into the Transformer layer. The general form of Adapter Tuning can be represented as:

$$\tilde{x} \leftarrow x + f(x \cdot \mathcal{W}^{\text{down}}) \cdot \mathcal{W}^{\text{up}} \quad (1)$$

where $x \in \mathbb{R}^d$ represents the input of the adapter, f is the activation function, $\mathcal{W}^{\text{down}} \in \mathbb{R}^{d \times r}$ and $\mathcal{W}^{\text{up}} \in \mathbb{R}^{r \times d}$ denote the linear layers for down-projection and up-projection, respectively. r is the bottleneck dimension, satisfying $r \ll d$, which allows for a reduction in the number of parameters in the adapter. Increasing r can enhance the performance of the adapter but also increases the total number of parameters. SparseAdapter [30] further exploits the high efficiency of parameters by pruning $\mathcal{W}^{\text{down}}$ and \mathcal{W}^{up} before tuning. In our work, we split the standard adapter into N sparse adapter experts $\mathcal{W}^{\text{down}} = \{\mathcal{W}_i^{\text{down}}\}_{i=1}^N$, $\mathcal{W}^{\text{up}} = \{\mathcal{W}_i^{\text{up}}\}_{i=1}^N$, and stochastically activate one of them during training for adaptation:

$$\tilde{x} \leftarrow x + f(x \cdot \mathcal{W}_i^{\text{down}}) \cdot \mathcal{W}_j^{\text{up}} \quad (2)$$

where $i, j \in \{1, \dots, N\}$, representing the stochastic selection of N experts.

3.2 Sparse Adapter Splitting

To make the most of all the parameters within a single adapter, we first split the standard adapter into multiple sparse adapters, as illustrated in Figure 1(c). As all parameters in the adapter need to be updated, unlike [30], we do not adopt the task-specific pruning mechanism but instead employ a random splitting method to achieve as balanced grouping as possible, which also avoids the additional overhead of gradient computation based on downstream tasks before fine-tuning. Given the parameter of adapter $\mathcal{W} \in \mathbb{R}^{d \times r}$, we first generate an initial score $\mathcal{S} \sim \text{Uniform}(0, 1) \in \mathbb{R}^{d \times r}$. Then, we split \mathcal{W} into N non-overlapping sparse adapters $\mathcal{W}_i : i \in \{1, \dots, N\}$ by \mathcal{S} . Denoting the i -th N -quantile of all values in the matrix \mathcal{S} as $s_i : i \in \{1, \dots, N\}$, we obtain N sparse masks \mathcal{M}_i as follows:

$$\mathcal{M}_i \leftarrow \mathbb{I}[s_{i-1} \leq \mathcal{S} < s_i] \quad (3)$$

where \mathbb{I} represents an all-ones matrix, and $s_0 = 0$.

Once the masks are calculated, sparse gradient updating is performed according to the following form:

$$\mathcal{W}'_i \leftarrow \mathcal{W}_i + \varepsilon \nabla \mathcal{L}(\mathcal{W}_i) \odot \mathcal{M}_i \quad (4)$$

where ε represents the update step size, and $\nabla \mathcal{L}(\mathcal{W}_i)$ denotes the gradient of the task loss with respect to \mathcal{W}_i . In this way, the positions with a mask value of 0 have their gradients filtered to 0, thereby freezing the corresponding parameters and achieving sparse training for the adapter. Consequently, we obtain N independent sparse adapters.

3.3 Stochastic Activation Tuning

With multiple sparse adapters, each can be treated as an expert, allowing for mixed training. Traditional MoE methods [67, 84] involve a routing mechanism, introducing additional computation and load imbalance. Considering that Adapter Tuning itself serves as a parameter-efficient method, and inspired by [73, 86], in the training process of MoSA, we also adopt a completely stochastic activation mechanism, which has been demonstrated to be simple yet effective in the following experiments. Given two partitioned parameter sets $\mathscr{W}^{\text{down}}$ and \mathscr{W}^{up} , for each batch of data, we randomly sample one module $\mathcal{W}_i^{\text{down}} \in \mathscr{W}^{\text{down}}, \mathcal{W}_j^{\text{up}} \in \mathscr{W}^{\text{up}}$ from each set to form an adapter $\mathcal{W} = \{\mathcal{W}_i^{\text{down}}, \mathcal{W}_j^{\text{up}}\}$, as shown in Equation (2). This activation mechanism ensures consistency in parameters and computational load with standard Adapter Tuning during training. Additionally, activating different sparse modules each time enables the model to learn different representations, thereby increasing the model capacity.

Hierarchical sparse strategy. Although the MoE system enhances the model capacity, the sparse activation also reduces the amount of data seen by individual experts, resulting in suboptimal performance, especially when training data for downstream tasks is limited. The pre-pruning and sparse training methods can mitigate this data dilution issue to a certain extent. Building upon this, we further propose a hierarchical sparse strategy. The adapter module consists of two parts: the down-projection layer and the up-projection layer. We keep the down-projection layer as a dense matrix, *i.e.* $\mathscr{W}^{\text{down}} = \mathcal{W}^{\text{down}}$, and only introduce sparsity in the up-projection layer, *i.e.* $\mathscr{W}^{\text{up}} = \{\mathcal{W}_i^{\text{up}}\}_{i=1}^N$. This adaptation process can be expressed as:

$$\tilde{x} \leftarrow x + f(x \cdot \mathcal{W}^{\text{down}}) \cdot \mathcal{W}_i^{\text{up}} \quad (5)$$

The dense down-projection layer provides robust intermediate features by receiving all training data, while multiple sparse up-projection layers map features to different subspaces, enhancing the performance on downstream tasks. Ablation experiments demonstrate the effectiveness of this hierarchical sparse strategy.

Deep feature alignment. Like [86] and [73], we also apply consistency regularization to ensure that different experts provide similar results for the same task. However, considering that different sparse adapters need to be merged after tuning, we further propose a deep feature alignment strategy to ensure that model parameters are not incompatible when merged. Given that deep features in neural networks are generally universal, while shallow features are typically task-specific, to strike a balance between model capacity and consistency, we align only the deep features of the model. Specifically, for a neural network with L layers, we align the features extracted by different experts in the first $L/2$ layers. The overall optimization objective is formulated as follows:

$$\mathcal{L}(x, y) = \text{CE}(p_1, y) + \frac{\alpha}{2} (\text{KL}(p_1 \| p_2) + \text{KL}(p_2 \| p_1)) + \beta \sum_{i=1}^{L/2} \text{MSE}(f_1^i, f_2^i) \quad (6)$$

where p_1, p_2 represent the predicted probabilities after two stochastic forward passes of x , and f_1^i, f_2^i represent the intermediate features in the i -th layer. Here,

CE is the cross-entropy loss, KL is the Kullback–Leibler divergence and MSE is the mean square error. α and β are hyper-parameters that control the weight of regularization terms, which are simply set to 1.0 in our main experiments.

3.4 Jigsaw-like Adapter Merging

During inference, we merge the trained multiple sparse adapters like puzzle pieces into a complete adapter, as illustrated in Figure 2. The merging process can be expressed as follows:

$$\overline{\mathcal{W}}[\mathcal{M}_i > 0] \leftarrow \mathcal{W}_i[\mathcal{M}_i > 0] \quad (7)$$

Here, \mathcal{M}_i represents the sparse mask for \mathcal{W}_i from Equation (4), and $\overline{\mathcal{W}}$ represents the merged complete projection layer weight. After merging, the inference phase can be represented as:

$$\tilde{x} \leftarrow x + f(x \cdot \overline{\mathcal{W}^{\text{down}}} \cdot \overline{\mathcal{W}^{\text{up}}}) \quad (8)$$

Experiments demonstrate that the merged adapter outperforms stochastic activation during inference.

4 Experiments

We evaluate MoSA across a series of downstream recognition tasks, spanning various model scales, architectures, and PEFT methods. We first describe our experimental setup in Section 4.1. Subsequently, we present the main experimental results in Section 4.2. Furthermore, we demonstrate the performance of MoSA applied to different backbone scales and PEFT methods in Section 4.3. In addition, we conduct extensive ablation experiments in Section 4.4 to verify the effectiveness of each component in our design. Finally, we provide t-SNE visualization results in Section 4.5.

4.1 Experimental Setup

Pre-trained backbones. We experiment with two Transformer architectures in vision: ViT [15] and Swin Transformer [51]. In our experiments, all models are pre-trained on ImageNet-21k [66]. We adhere to the original configurations of these models, such as the number of image patches divided and the inclusion of the [CLS] token, etc. More details can be found in Appendix.

Baselines. We compare our MoSA with other Adapter Tuning methods and commonly used fine-tuning strategies:

- **Full fine-tuning:** fully update the whole backbone.
- **Linear probing:** fix the model backbone and only update the classifier.
- **BitFit (Bias) [80]:** fine-tune all the bias terms in the pre-trained backbone.
- **Visual prompt tuning (VPT) [36]:** add learnable embeddings as prompts to modify the input, in two versions: shallow (insert prompts only into the first layer) and deep (introduce prompts at every layer).

- **AdaptFormer [7]**: insert bottleneck modules with residual connections to the feed-forward network (FFN) of each Transformer layer.
- **SparseAdapter [30]**: prune the standard adapter before tuning and update the remaining parameters via masks.

Downstream tasks. We evaluate MoSA against other baselines on the following three collections of datasets:

- **FGVC**: This benchmark consists of 5 Fine-Grained Visual Classification tasks, including CUB-200-2011 [72], NABirds [70], Oxford Flowers [59], Stanford Dogs [13], and Stanford Cars [19], which are representative examples of this category. We directly adapt the public split for training and validation sets if available, or we just follow the splits in [36].
- **VTAB**: VTAB-1k [82] benchmark consists of 19 visual classification tasks from 3 diverse domains: *Natural*, *Specialized* and *Structured*. Each task contains only 1000 training examples, but potentially spanning up to 397 classes, poses a significant challenge.
- **GICD**: We also collect a benchmark of 3 General Image Classification Datasets, including CIFAR-100 [41], Aircraft [56] and Food-101 [4], to demonstrate the efficiency of MoSA. All the datasets comprise around 100 categories, each containing at least 10,000 images, all of which are common objects in natural scenes.

Implementation details. For all datasets, we only process the images with a randomly resized crop to 224×224 and a random horizontal flip for data augmentation, instead of other strong augmentation and regularization strategies, like mixup [83] and cutmix [77]. We adopt the AdamW [53] optimizer to fine-tune the pre-trained model for 100 epochs, with a linear warm-up of the learning rate for the first 10 epochs. For a fair comparison, we set the general hyperparameters to be the same in all Adaptor Tuning methods, including our MoSA. All experiments are conducted using the PyTorch [63] library on NVIDIA V100 and A100 GPUs. More implementation details can be found in Appendix.

4.2 Main Results

We provide a comprehensive evaluation of the effectiveness of our MoSA by comparing it with other baselines across 3 sets of up to 27 different datasets. In the following experiments, Top-1 accuracy (%) is used to evaluate the performance of the methods on the respective datasets, and the number (M) of extra parameters (trainable parts excluding the classifier) is used to assess the efficiency of the methods. The best accuracy is highlighted in **bold**, while the second one is underlined. The results of our method is highlighted with a red background.

Fine-grained classification performance. We first evaluate the effectiveness of our method on 5 widely used fine-grained visual classification tasks with ViT-B/16 [15] backbone. As shown in Table 1, our MoSA beats other baselines, including full fine-tuning, by a significant margin. Across the 5 downstream tasks, MoSA achieves an average accuracy of 89.90%, surpassing full fine-tuning

Table 1: Results on FGVC with ViT-B/16 backbone pre-trained on ImageNet-21K

Method \ Dataset	CUB-200 -2011	NABrids	Oxford Flowers	Stanford Dogs	Stanford Cars	Mean Acc. (%)	Mean Params. (M)
Full fine-tuning	87.3	82.7	98.8	89.4	84.5	88.54	85.80
Linear probing	85.3	75.9	97.9	86.2	51.3	79.32	0.00
BitFit [80]	88.4	84.2	98.8	91.2	79.4	88.40	0.10
VPT-shallow [36]	86.7	78.8	98.4	90.7	68.7	84.62	0.27
VPT-deep [36]	<u>88.5</u>	84.2	<u>99.0</u>	90.2	<u>83.6</u>	<u>89.11</u>	0.84
AdaptFormer [7]	87.4	84.8	<u>99.0</u>	90.7	81.0	88.58	1.54
SparseAdapter [30]	87.8	<u>85.1</u>	98.9	<u>91.4</u>	80.3	88.70	0.39
MoSA (Ours)	89.3	85.7	99.2	91.9	83.4	89.90	1.54

Table 2: Results on VTAB with ViT-B/16 backbone pre-trained on ImageNet-21K

Method \ Dataset	Natural	Specialized	Structured	Mean Acc. (%)	Mean Params. (M)
Full fine-tuning	75.88	83.36	47.64	68.96	85.80
Linear probing	68.93	77.16	26.84	57.64	0.00
BitFit [80]	73.30	78.25	44.09	65.21	0.10
VPT-shallow [36]	76.81	79.66	46.98	64.85	0.11
VPT-deep [36]	<u>78.48</u>	82.43	54.98	69.42	0.98
AdaptFormer [7]	78.42	<u>83.41</u>	49.17	<u>70.33</u>	0.30
SparseAdapter [30]	77.58	81.99	48.26	69.28	0.08
MoSA (Ours)	79.86	84.03	<u>50.28</u>	71.39	0.30

and AdaptFormer [7] by 1.36% and 1.32%, respectively, while maintaining the same number of trainable parameters as [7]. Interestingly, SparseAdapter [30], with fewer trainable parameters just through pruning, outperforms the standard adapter by 0.12% on average, demonstrating the parameter redundancy in adapters for visual tasks. However, the high sparsity level results in ineffective utilization of most parameters in the adapter, limiting the overall performance gain. MoSA increases model capacity by mixed training of multiple sparse adapters, achieving an additional improvement of 1.20%. Experiments show that our method enhances the performance of existing methods without introducing extra parameters or computation, maximizing the potential of adapters.

Low-resource visual adaptation performance. We also compare our method with other fine-tuning approaches on VTAB, which contains 19 diverse downstream tasks with only 1000 training samples per task, making it extremely challenging. Previous stochastically activated MoE methods, like [86], suffer from severe performance degradation when training data is insufficient. However, our MoSA overcomes this issue with its sparse training paradigm and hierarchical sparse strategy. The results in Table 2 demonstrate that MoSA outperforms all

Table 3: Results on GICD with ViT-B/16 backbone pre-trained on ImageNet-21K

Method \ Dataset	Dataset			Mean	Mean
	CIFAR-100	Aircraft	Food-101	Acc. (%)	Params. (M)
Full fine-tuning	89.12	70.93	<u>90.96</u>	83.67	85.80
Linear probing	85.95	45.06	88.14	73.05	0.00
BitFit [80]	91.69	68.71	89.59	83.33	0.10
AdaptFormer [7]	<u>91.86</u>	<u>71.71</u>	90.89	<u>84.82</u>	1.19
SparseAdapter [30]	91.20	67.15	89.37	82.57	0.30
MoSA (Ours)	92.22	72.14	91.17	85.18	1.19

other baselines by updating only 0.35% (0.30M in 85.80M) of the pre-trained backbone parameters. Specifically, across 3 domains in VTAB, MoSA surpasses full fine-tuning by 3.98%, 0.67% and 2.64%, while outperforming the second-best AdaptFormer by 1.44%, 0.62% and 1.11%, providing strong evidence for the effectiveness of our design.

General large-scale classification performance. To further evaluate the generality of our method, we compare MoSA with other fine-tuning methods on 3 general classification tasks, as shown in Table 3. MoSA outperforms all baselines, including full fine-tuning, on all datasets. Specifically, compared to AdaptFormer and full fine-tuning, MoSA achieves an average accuracy improvement of 1.51% and 0.36%, respectively, without introducing any additional parameters. It is worth noting that SparseAdapter performs poorly on this benchmark, exhibiting an accuracy drop of 2.25% compared to the standard adapter. This is attributed to the fact that the three datasets in GICD contain relatively sufficient training data, mitigating the advantages of sparsity. However, our method, through multiple sparse adapter experts, demonstrates robust performance in scenarios with both abundant and limited training data, outperforming SparseAdapter by 2.61%, which proves the soundness of our design.

4.3 Extended Results on Different Backbone Scales and LoRA

In this section, we validate the performance of MoSA on different backbone scales and PEFT methods. More experiments on different model architectures (*e.g.* Swin Transformer) and adapter structures can be found in Appendix.

MoSA on different backbone scales. Here we evaluate MoSA with a larger backbone ViT-L/16 (303.3M *vs.* 85.8M ViT-B/16). The results in Table 4 indicate that, with the increase in backbone scale, the performance of the standard adapter cannot surpass full fine-tuning (89.70% *vs.* 90.16%). Sparse training could improve the performance of adapters, leading by 0.58% and 0.12% over the standard adapter and full fine-tuning, respectively. Our MoSA further enhances the performance by 0.78%, outperforming full fine-tuning by a large margin. This experiment thoroughly demonstrates the importance of sparse training as the scale of pre-trained models increases.

Table 4: Results on FGVC with ViT-L/16 backbone pre-trained on ImageNet-21K

Method \ Dataset	CUB-200 -2011	NABrids	Oxford Flowers	Stanford Dogs	Stanford Cars	Mean Acc. (%)	Mean Params. (M)
Full fine-tuning	88.3	85.9	96.7	93.1	86.8	90.16	303.30
Linear probing	84.7	78.9	97.4	89.6	55.1	81.14	0.00
BitFit [80]	88.5	86.4	98.8	93.5	83.2	90.08	0.27
AdaptFormer-64 [7]	89.3	86.3	98.8	93.2	80.9	89.70	3.17
SparseAdapter-64 [30]	<u>89.4</u>	<u>86.8</u>	<u>99.0</u>	<u>93.9</u>	82.3	<u>90.28</u>	0.79
MoSA-64 (Ours)	89.7	87.2	99.4	94.5	<u>84.9</u>	91.06	3.17

Table 5: Results on FGVC with LoRA

Method \ Dataset	CUB-200 -2011	NABrids	Oxford Flowers	Stanford Dogs	Stanford Cars	Mean Acc. (%)	Mean Params. (M)
LoRA-16 [34]	87.2	83.5	98.6	89.3	83.7	88.44	0.59
SparseLoRA-16 [30]	87.4	84.9	98.9	91.1	79.9	88.44	0.15
MoSL-16 (Ours)	89.0	85.6	99.3	91.8	83.9	89.92	0.59

MoSA on different PEFT methods. To demonstrate the generality of our approach, we choose another widely used PEFT method, namely LoRA [34]. LoRA achieves parameter-efficient fine-tuning by applying a low-rank decomposition to the weight updates of linear layers. During inference, the additional modules could be merged into the pre-trained model parameters, resulting in zero extra overhead during inference. In Table 5, we compare the LoRA version sparse adapter (namely SparseLoRA) and our MoSA (namely MoSL) with the standard LoRA, with the rank of all LoRA modules set to 16. Our MoSL outperforms both the standard and sparse versions of LoRA, achieving an improvement of 1.48%, further confirming the effectiveness and rationality of our design.

4.4 Ablation Study

We conduct comprehensive ablation studies to verify the effectiveness of each component in our MoSA design. All ablation experiments are performed on FGVC with ViT-B backbone, and the performances of different strategies are measured using mean accuracy over the datasets. The best component choice, which is also used in the main results, is highlighted with a **green** background. **Hierarchical sparse strategy.** The MoE system increases the model capacity, while the sparse gating mechanism also leads to a decrease in the amount of data each expert encounters, resulting in suboptimal performance particularly when training data for downstream tasks is limited. In order to address this issue, we propose a hierarchical sparse strategy, and the results in Table 6 demonstrate the effectiveness of this design. Applying the sparse strategy to both the down-projection and up-projection layer only achieves an accuracy of 88.91%, slightly (0.33%) ahead of Adaptformer (dense down-projection and up-projection layer). However, with the hierarchical sparse strategy, we preserve the down-projection layer as a dense matrix while sparsely splitting the up-projection layer. In this

Table 6: Hierarchical sparse strategy

Strategy	Mean Acc. (%)
dense down + dense up	88.58
sparse down + sparse up	88.91
dense down + sparse up	89.90

Table 7: Consistency regularization

Regularization	Mean Acc. (%)
none	88.93
consistency	89.25
consistency + alignment	89.90

Table 8: Different alignment strategies

Alignment position	none	shallow	deep	all
Mean Acc. (%)	89.25	89.90	88.84	88.79

Table 9: Impact of expert number

Expert number	1	2	3	4	5	8
Mean Acc. (%)	88.58	89.59	89.42	89.43	89.05	88.57

Table 10: Different inference mechanisms and corresponding efficiency

Mechanism	FLOPs	Mean Acc. (%)
fixed	1×	88.42
stochastic	1×	89.27
ensemble	$N \times$	88.63
merge	1×	89.90

way, MoSA outperforms Adaptformer by a large margin (89.90% *vs.* 88.58%), demonstrating the importance of this hierarchical strategy.

Consistency regularization and feature alignment. The mechanism of stochastic activation may lead to significant discrepancies among different experts, which can have adverse effects on the sparse module merging. In Table 7, we investigate the impact of regularization constraints in the training of MoSA. Without any regularization, our method achieves an accuracy of 88.93%. Applying consistency regularization on the final outputs of the model results in an improvement of 0.32%. And deep alignment of features extracted by different experts can further improve the accuracy by 0.65%. We also explore the impact of different feature alignment positions on model performance. As shown in Table 8, performing alignment solely at shallow layers (closer to the input) can lead to a 0.65% improvement. In contrast, executing alignment at deep layers (closer to the output) results in a 0.41% decrease, attributable to sub-module collapse.

Expert number. To evaluate the compatibility between sparse training and MoE, we vary the number of splits in the adapters of MoSA during training, ranging from 1 to 5 and 8. The results are presented in Table 9. When the number of splits is set to 1, our method degrades to AdaptFormer. We can see that when the number of experts is between 2 and 5, indicating a sparsity level between 20% and 50% for the adapters, MoSA consistently achieves good performance. However, when the number of experts increases to 8, the performance experiences a noticeable decline due to excessive sparsity.

Merging *vs.* ensembling. During inference, we merge multiple sparse adapters to form a complete one. However, it has been pointed out that stochastic activation during inference can also achieve good performance [86]. So we compare various inference methods, including fixed activation, stochastic activation, logits ensembling, and parameter merging. Results are presented in Table 10. It can be observed that fixed activation has the lowest accuracy, reaching only 88.41% on

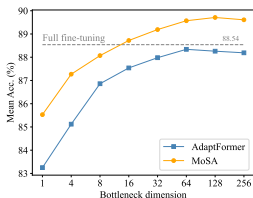


Fig. 3: Impact of adapter bottleneck dimensions

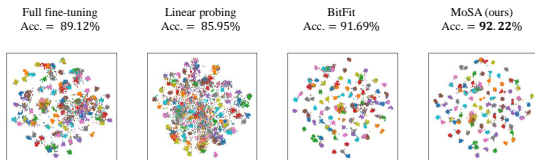


Fig. 4: t-SNE visualization on CIFAR-100

average. In comparison, stochastic activation achieves an improvement of 0.85%. Logits ensembling also leads to a certain improvement over fixed activation, but the increase of only 0.21% comes at the cost of N times computational complexity (N refers to the expert number), significantly reducing the inference speed. Finally, our parameter merging method achieves the best performance without any additional computation, further enhancing 0.63% over stochastic activation.

Adapter bottleneck dimension. Figure 3 shows the impact of bottleneck dimensions of the adapter in AdaptFormer and MoSA. Overall, the performance shows an increasing trend followed by a decline as the number of trainable parameters increases. Across all bottleneck dimensions, MoSA consistently outperforms AdaptFormer, and our method can even surpass full fine-tuning with a bottleneck dimension of only 16. It is worth noting that the performance of AdaptFormer starts to decline when the bottleneck dimension exceeds 64, while in our method, this turning point occurs at 128. This indicates that our design can more effectively utilize all parameters within the adapter.

4.5 Visualization

Here, we provide t-SNE visualizations to show the feature distribution of different methods on the CIFAR-100 dataset. The results are shown in Figure 4. We can observe that our MoSA achieves better feature clustering compared to full fine-tuning and other PEFT baselines.

5 Conclusion

In this paper, we focus on the Adapter Tuning method in parameter-efficient fine-tuning and propose MoSA to improve the performance of standard adapters without any extra parameters or computation. Recognizing that standard adapters still suffer from parameter redundancy, we combine sparse training with multiple stochastically activated experts to fully utilize all parameters within the adapters. Comprehensive experiments on a total of 27 datasets show that MoSA consistently outperforms all other baselines, achieving state-of-the-art performance in Adapter Tuning. We hope that our work could inspire researchers to reconsider the issue of parameter redundancy in adapters and make further advancements towards more efficient PEFT methods.

A Dataset Details

Here, we describe the details of all datasets used to validate MoSA. The number of classes and the train/valid/test splits for each dataset are shown in Table 11.

- **FGVC**: Fine-Grained Visual Classification (FGVC) benchmark consists of 5 downstream tasks, which are CUB-200-2011 [72], NABirds [70], Oxford Flowers [59], Stanford Dogs [13] and Stanford Cars [19]. Each task contains more than 100 classes and a few thousand images.
- **VTAB**: Visual Task Adaptation Benchmark [82] (VTAB) contains 19 visual classification tasks grouped into 3 domains: (1) *Natural* - tasks with natural images captured by standard cameras; (2) *Specialized* - tasks with images captured via specialized equipment, *e.g.* medical camera and satellite sensor; (3) *Structured* - tasks with images synthesized from simulated environments, which require geometric comprehension like object counting and depth estimation. Each task of VTAB contains only 1000 training samples, but may span up to 397 classes with several thousand testing samples, making it highly challenging.
- **GICD**: General Image Classification Datasets (GICD) benchmark consists of 3 general classification tasks, which are CIFAR-100 [41], Aircraft [56] and Food-101 [4]. All the tasks comprise around 100 classes, each containing at least 10,000 images, all of which are common objects in natural scenes.

B Implementation Details

In Table 12, we summarize all experimental configurations with Adapter Tuning and LoRA. For other baselines, we just follow [36]. Following the linear scaling rule [10, 22, 28, 42], the learning rate is set as $base_lr \times b/256$, where b is the batch size and $base_lr$ is chosen from the range specified in Table 12.

C More Experimental Results

In this section, we validate MoSA on different backbone architectures and adapter structures. We also show the pre-task results for MoSA with ViT-B/16 on VTAB-1k. Similar to the main text, Top-1 accuracy (%) is used to evaluate the performance of the methods on the respective datasets, and the number (M) of extra parameters (trainable parts excluding the classifier) is used to assess the efficiency. The best accuracy is highlighted in **bold**, while the second one is underlined. The results of our method is highlighted with a red background.

MoSA on different model architectures. In addition to the standard ViT, we also experiment with another hierarchical vision Transformer, Swin-B [51], to demonstrate the effectiveness of MoSA. Similar to ViT, we can easily apply MoSA to Swin. As shown in Table 13, due to the strong feature extraction capability of this model architecture, full fine-tuning performs well on Swin, while

Table 11: Details of all datasets used to validate MoSA.

Dataset		#Classes	Train	Val	Test
Fine-Grained Visual Classification (FGVC)					
CUB-200-2011 [72]		200	5,394	600	5,794
NABirds [70]		555	21,536	2,393	24,633
Oxford Flowers [59]		102	1,020	1,020	6,149
Stanford Dogs [13]		120	10,800	1,200	8,580
Stanford Cars [19]		196	7,329	815	8,041
Visual Task Adaptation Benchmark (VTAB) [82]					
Natural	CIFAR-100 [41]	100			10,000
	Caltech101 [17]	102			6,084
	DTD [12]	47			1,880
	Flowers102 [59]	102	800/1000	200	6,149
	Pets [62]	37			3,669
	SVHN [78]	10			26,032
	Sun397 [74]	397			21,750
Specialized	Patch Camelyon [71]	2			32,768
	EuroSAT [32]	10	800/1000	200	5,400
	Resisc45 [11]	45			6,300
	Retinopathy [23]	5			42,670
Structured	Clevr/count [38]	8			15,000
	Clevr/distance [38]	6			15,000
	DMLab [3]	6			22,735
	KITTI/distance [20]	4	800/1000	200	711
	dSprites/location [57]	16			73,728
	dSprites/orientation [57]	16			73,728
	SmallNORB/azimuth [43]	18			12,150
	SmallNORB/elevation [43]	9			12,150
General Image Classification Datasets (GICD)					
CIFAR-100 [41]		100	50,000	-	10,000
Aircraft [56]		100	3,334	3,333	3,333
Food-101 [4]		101	75,750	-	25,250

Table 12: Implementation details for Adapter Tuning and LoRA.

Configuration	Value
Optimizer	AdamW [53]
Base learning rate range	{0.01, 0.005, 0.001, 0.0005, 0.0001}
Weight decay range	{0.01, 0.0}
Learning rate schedule	cosine decay [52]
Batch size	128 (ViT-B/16, Swin-B), 64 (ViT-L/16)
Warmup epoch	10
Total epoch	100 (ViT-B/16, Swin-B), 50 (ViT-L/16)
Augmentation	RandomResizedCrop [28], RandomHorizontalFlip

Table 13: Results on FGVC with Swin-B backbone pre-trained on ImageNet-21K.

Method \ Dataset	CUB-200 -2011	NABrids	Oxford Flowers	Stanford Dogs	Stanford Cars	Mean Acc. (%)	Mean Params. (M)
Full fine-tuning	88.2	87.8	99.0	85.5	90.2	<u>90.14</u>	86.74
Linear probing	87.8	83.8	98.8	84.7	69.2	84.86	0.00
BitFit [80]	88.4	85.2	99.2	85.3	83.4	88.30	0.20
AdaptFormer-64 [7]	<u>89.7</u>	<u>87.7</u>	99.3	86.0	<u>87.7</u>	90.08	1.55
SparseAdapter-64 [30]	<u>89.7</u>	<u>87.4</u>	<u>99.4</u>	<u>87.1</u>	86.8	90.08	0.39
MoSA-64 (Ours)	90.6	87.8	99.6	88.3	87.3	90.72	1.55

Table 14: Results on FGVC with different adapter structures.

Method \ Dataset	CUB-200 -2011	NABrids	Oxford Flowers	Stanford Dogs	Stanford Cars	Mean Acc. (%)	Mean Params. (M)
Adapter-Pfeiffer [64]	84.5	81.3	97.9	88.8	76.7	85.84	1.21
SparseAdapter-Pfeiffer [30]	86.7	83.9	98.5	90.0	77.6	87.34	0.30
MoSA-Pfeiffer (Ours)	89.3	85.5	99.2	91.6	79.6	89.04	1.21
Adapter-Houlsby [33]	87.5	81.9	97.9	89.0	75.7	86.40	2.38
SparseAdapter-Houlsby [30]	87.5	83.3	98.9	90.1	78.7	87.70	0.59
MoSA-Houlsby (Ours)	89.3	86.2	99.3	92.1	80.4	89.46	2.38

other PEFT methods show suboptimal performance. It’s worth noting that our MoSA is the only method that outperforms full fine-tuning on Swin (90.72% *vs.* 90.14%), indicating that MoSA consistently adapts various vision Transformers to downstream tasks and improves performance.

MoSA on different adapter structures. As a supplement, we apply MoSA to two different adapter structures: Pfeiffer [64] and Houlsby [33]. Both Pfeiffer and Houlsby use a sequential connection for adapter design, with Pfeiffer incorporating the adapters only after the FFN layers, while Houlsby includes the adapters after both the Attention and FFN layers. The performance comparison on the two adapter structures is shown in Table 14. In this experiment, the bottleneck dimension for all adapters is set to 64. It can be observed that on both structures, sparse training brings improvements of 1.50% and 1.30% over the standard adapter, and the corresponding versions of our MoSA further yield performance gains of 1.70% and 1.76%.

Per-task results for MoSA on VTAB-1k. Table 15 shows the per-task results of MoSA on VTAB-1k. It can be seen that MoSA outperforms full fine-tuning on 13 tasks of VTAB, the highest among all PEFT methods. Additionally, MoSA also surpasses full fine-tuning (68.25% *vs.* 65.57%) and other baselines (AdaptFormer 67.16%) in the average accuracy across 19 tasks.

Table 15: Per-task results on VTAB-1k with ViT-B/16 pre-trained on ImageNet-21K.

Method \ Dataset	Natural										Specialized					Structured						
	CIFAR-100	Cattech101	DTD	Flowers102	Pets	SVHN	Sum397	Mean	Patch Camelyon	EuroSAT	Resisc45	Retinopathy	Mean	Clevr/count	Clevr/distance	DMLab	KITTI/distance	dSprites/loc	dSprites/ori	SmallNORB/azi	SmallNORB/ele	Mean
Full fine-tuning	68.9	87.7	64.3	97.2	86.9	87.4	38.8	75.88	79.7	<u>95.7</u>	84.2	73.9	83.36	56.3	<u>58.6</u>	<u>41.7</u>	65.5	<u>57.5</u>	<u>46.7</u>	25.7	29.1	65.57
Linear probing	63.4	85.0	64.3	97.0	86.3	36.6	51.0	68.93	78.5	87.5	68.6	74.0	77.16	34.3	30.6	33.2	55.4	12.5	20.0	9.6	19.2	53.00
BitFit [80]	72.8	87.0	59.2	97.5	85.3	59.9	51.4	73.30	78.7	91.6	72.9	69.8	78.25	61.5	55.6	32.4	55.9	66.6	40.0	15.7	25.1	62.05
VPT-shallow [36]	77.7	86.9	62.6	97.5	87.3	74.5	51.2	76.81	78.2	92.0	75.6	72.9	79.66	50.5	<u>58.6</u>	40.5	67.1	<u>68.7</u>	36.1	20.2	34.1	64.85
VPT-deep [36]	78.8	<u>90.8</u>	65.8	98.0	88.3	78.1	49.6	<u>78.48</u>	<u>81.8</u>	96.1	<u>83.4</u>	68.4	82.43	68.5	60.0	46.5	72.8	73.6	47.9	32.9	37.8	69.42
AdaptFormer [7]	78.9	90.0	67.0	<u>98.7</u>	89.0	72.2	<u>53.2</u>	78.42	81.5	<u>95.7</u>	81.2	75.2	83.41	70.6	57.4	39.3	70.6	54.5	42.4	25.3	33.3	67.16
SparseAdapter [30]	79.1	89.2	65.7	98.6	89.3	68.5	52.5	77.58	79.5	94.7	79.4	74.4	81.99	70.2	56.9	37.8	70.9	51.3	41.3	25.2	32.5	66.16
MoSA (Ours)	79.7	91.5	<u>66.2</u>	98.8	89.7	79.0	53.4	79.86	83.4	95.6	82.0	<u>75.1</u>	84.03	71.5	58.1	40.7	70.2	57.8	43.6	26.5	34.0	68.25

References

1. Ansell, A., Ponti, E.M., Korhonen, A., Vulić, I.: Composable sparse fine-tuning for cross-lingual transfer. arXiv preprint arXiv:2110.07560 (2021)
2. Bai, Y., Geng, X., Mangalam, K., Bar, A., Yuille, A., Darrell, T., Malik, J., Efros, A.A.: Sequential modeling enables scalable learning for large vision models. arXiv preprint arXiv:2312.00785 (2023)
3. Beattie, C., Leibo, J.Z., Teplyashin, D., Ward, T., Wainwright, M., Küttler, H., Lefrancq, A., Green, S., Valdés, V., Sadik, A., et al.: Deepmind lab. arXiv preprint arXiv:1612.03801 (2016)
4. Bossard, L., Guillaumin, M., Van Gool, L.: Food-101—mining discriminative components with random forests. In: Computer Vision—ECCV 2014: 13th European Conference, Zurich, Switzerland, September 6–12, 2014, Proceedings, Part VI 13. pp. 446–461. Springer (2014)
5. Brown, T., Mann, B., Ryder, N., Subbiah, M., Kaplan, J.D., Dhariwal, P., Neelakantan, A., Shyam, P., Sastry, G., Askell, A., et al.: Language models are few-shot learners. *Advances in neural information processing systems* **33**, 1877–1901 (2020)
6. Chen, S., Jie, Z., Ma, L.: Llava-mole: Sparse mixture of lora experts for mitigating data conflicts in instruction finetuning mllms. arXiv preprint arXiv:2401.16160 (2024)
7. Chen, S., Ge, C., Tong, Z., Wang, J., Song, Y., Wang, J., Luo, P.: Adaptformer: Adapting vision transformers for scalable visual recognition. *Advances in Neural Information Processing Systems* **35**, 16664–16678 (2022)
8. Chen, T., Zhu, L., Ding, C., Cao, R., Zhang, S., Wang, Y., Li, Z., Sun, L., Mao, P., Zang, Y.: Sam fails to segment anything?—sam-adapter: Adapting sam in underperformed scenes: Camouflage, shadow, and more. arXiv preprint arXiv:2304.09148 (2023)
9. Chen, T., Kornblith, S., Norouzi, M., Hinton, G.: A simple framework for contrastive learning of visual representations. In: International conference on machine learning. pp. 1597–1607. PMLR (2020)
10. Chen, X., Xie, S., He, K.: An empirical study of training self-supervised vision transformers. In: CVF International Conference on Computer Vision (ICCV). pp. 9620–9629 (2021)
11. Cheng, G., Han, J., Lu, X.: Remote sensing image scene classification: Benchmark and state of the art. *Proceedings of the IEEE* **105**(10), 1865–1883 (2017)
12. Cimpoi, M., Maji, S., Kokkinos, I., Mohamed, S., Vedaldi, A.: Describing textures in the wild. In: Proceedings of the IEEE conference on computer vision and pattern recognition. pp. 3606–3613 (2014)
13. Dataset, E.: Novel datasets for fine-grained image categorization. In: First Workshop on Fine Grained Visual Categorization, CVPR. Citeseer. Citeseer. Citeseer (2011)
14. Ding, N., Qin, Y., Yang, G., Wei, F., Yang, Z., Su, Y., Hu, S., Chen, Y., Chan, C.M., Chen, W., et al.: Delta tuning: A comprehensive study of parameter efficient methods for pre-trained language models. arXiv preprint arXiv:2203.06904 (2022)
15. Dosovitskiy, A., Beyer, L., Kolesnikov, A., Weissenborn, D., Zhai, X., Unterthiner, T., Dehghani, M., Minderer, M., Heigold, G., Gelly, S., et al.: An image is worth 16x16 words: Transformers for image recognition at scale. arXiv preprint arXiv:2010.11929 (2020)
16. Dou, S., Zhou, E., Liu, Y., Gao, S., Zhao, J., Shen, W., Zhou, Y., Xi, Z., Wang, X., Fan, X., et al.: Loramoe: Revolutionizing mixture of experts for maintaining world knowledge in language model alignment. arXiv preprint arXiv:2312.09979 (2023)

17. Fei-Fei, L., Fergus, R., Perona, P.: One-shot learning of object categories. *IEEE transactions on pattern analysis and machine intelligence* **28**(4), 594–611 (2006)
18. Gao, C., Chen, K., Rao, J., Sun, B., Liu, R., Peng, D., Zhang, Y., Guo, X., Yang, J., Subrahmanian, V.: Higher layers need more lora experts. *arXiv preprint arXiv:2402.08562* (2024)
19. Gebru, T., Krause, J., Wang, Y., Chen, D., Deng, J., Fei-Fei, L.: Fine-grained car detection for visual census estimation. In: *Proceedings of the AAAI Conference on Artificial Intelligence*. vol. 31 (2017)
20. Geiger, A., Lenz, P., Stiller, C., Urtasun, R.: Vision meets robotics: The kitti dataset. *The International Journal of Robotics Research* **32**(11), 1231–1237 (2013)
21. Gou, Y., Liu, Z., Chen, K., Hong, L., Xu, H., Li, A., Yeung, D.Y., Kwok, J.T., Zhang, Y.: Mixture of cluster-conditional lora experts for vision-language instruction tuning. *arXiv preprint arXiv:2312.12379* (2023)
22. Goyal, P., Dollár, P., Girshick, R., Noordhuis, P., Wesolowski, L., Kyrola, A., Tulloch, A., Jia, Y., He, K.: Accurate, large minibatch sgd: Training imagenet in 1 hour. *arXiv preprint arXiv:1706.02677* (2017)
23. Graham, B.: Kaggle diabetic retinopathy detection competition report. *University of Warwick* pp. 24–26 (2015)
24. Guo, D., Rush, A.M., Kim, Y.: Parameter-efficient transfer learning with diff pruning. *arXiv preprint arXiv:2012.07463* (2020)
25. Han, C., Wang, Q., Cui, Y., Wang, W., Huang, L., Qi, S., Liu, D.: Facing the elephant in the room: Visual prompt tuning or full finetuning? *arXiv preprint arXiv:2401.12902* (2024)
26. Han, S., Liu, X., Mao, H., Pu, J., Pedram, A., Horowitz, M.A., Dally, W.J.: Eie: Efficient inference engine on compressed deep neural network. *ACM SIGARCH Computer Architecture News* **44**(3), 243–254 (2016)
27. He, H., Cai, J., Zhang, J., Tao, D., Zhuang, B.: Sensitivity-aware visual parameter-efficient fine-tuning. In: *Proceedings of the IEEE/CVF International Conference on Computer Vision*. pp. 11825–11835 (2023)
28. He, K., Chen, X., Xie, S., Li, Y., Dollár, P., Girshick, R.: Masked autoencoders are scalable vision learners. In: *Proceedings of the IEEE/CVF conference on computer vision and pattern recognition*. pp. 16000–16009 (2022)
29. He, K., Fan, H., Wu, Y., Xie, S., Girshick, R.: Momentum contrast for unsupervised visual representation learning. In: *Proceedings of the IEEE/CVF conference on computer vision and pattern recognition*. pp. 9729–9738 (2020)
30. He, S., Ding, L., Dong, D., Zhang, M., Tao, D.: Sparseadapter: An easy approach for improving the parameter-efficiency of adapters. *arXiv preprint arXiv:2210.04284* (2022)
31. He, X., Li, C., Zhang, P., Yang, J., Wang, X.E.: Parameter-efficient model adaptation for vision transformers. *arXiv preprint arXiv:2203.16329* (2022)
32. Helber, P., Bischke, B., Dengel, A., Borth, D.: Eurosat: A novel dataset and deep learning benchmark for land use and land cover classification. *IEEE Journal of Selected Topics in Applied Earth Observations and Remote Sensing* **12**(7), 2217–2226 (2019)
33. Houshy, N., Giurgiu, A., Jastrzebski, S., Morrone, B., De Laroussilhe, Q., Gesmundo, A., Attariyan, M., Gelly, S.: Parameter-efficient transfer learning for nlp. In: *International Conference on Machine Learning*. pp. 2790–2799. PMLR (2019)
34. Hu, E.J., Shen, Y., Wallis, P., Allen-Zhu, Z., Li, Y., Wang, S., Wang, L., Chen, W.: Lora: Low-rank adaptation of large language models. *arXiv preprint arXiv:2106.09685* (2021)

35. Jacobs, R.A., Jordan, M.I., Nowlan, S.J., Hinton, G.E.: Adaptive mixtures of local experts. *Neural computation* **3**(1), 79–87 (1991)
36. Jia, M., Tang, L., Chen, B.C., Cardie, C., Belongie, S., Hariharan, B., Lim, S.N.: Visual prompt tuning. In: *European Conference on Computer Vision*. pp. 709–727. Springer (2022)
37. Jie, S., Deng, Z.H.: Fact: Factor-tuning for lightweight adaptation on vision transformer. In: *Proceedings of the AAAI Conference on Artificial Intelligence*. vol. 37, pp. 1060–1068 (2023)
38. Johnson, J., Hariharan, B., Van Der Maaten, L., Fei-Fei, L., Lawrence Zitnick, C., Girshick, R.: Clevr: A diagnostic dataset for compositional language and elementary visual reasoning. In: *Proceedings of the IEEE conference on computer vision and pattern recognition*. pp. 2901–2910 (2017)
39. Karimi Mahabadi, R., Henderson, J., Ruder, S.: Compacter: Efficient low-rank hypercomplex adapter layers. *Advances in Neural Information Processing Systems* **34**, 1022–1035 (2021)
40. Kirillov, A., Mintun, E., Ravi, N., Mao, H., Rolland, C., Gustafson, L., Xiao, T., Whitehead, S., Berg, A.C., Lo, W.Y., et al.: Segment anything. *arXiv preprint arXiv:2304.02643* (2023)
41. Krizhevsky, A.: Learning multiple layers of features from tiny images. University of Toronto (05 2012)
42. Krizhevsky, A.: One weird trick for parallelizing convolutional neural networks. *arXiv preprint arXiv:1404.5997* (2014)
43. LeCun, Y., Huang, F.J., Bottou, L.: Learning methods for generic object recognition with invariance to pose and lighting. In: *Proceedings of the 2004 IEEE Computer Society Conference on Computer Vision and Pattern Recognition, 2004. CVPR 2004*. vol. 2, pp. II–104. IEEE (2004)
44. Lee, G., Jang, W., Kim, J.H., Jung, J., Kim, S.: Domain generalization using large pretrained models with mixture-of-adapters. *arXiv preprint arXiv:2310.11031* (2023)
45. Lester, B., Al-Rfou, R., Constant, N.: The power of scale for parameter-efficient prompt tuning. *arXiv preprint arXiv:2104.08691* (2021)
46. Li, X.L., Liang, P.: Prefix-tuning: Optimizing continuous prompts for generation. *arXiv preprint arXiv:2101.00190* (2021)
47. Lian, D., Zhou, D., Feng, J., Wang, X.: Scaling & shifting your features: A new baseline for efficient model tuning. *Advances in Neural Information Processing Systems* **35**, 109–123 (2022)
48. Liu, H., Tam, D., Muqeeth, M., Mohta, J., Huang, T., Bansal, M., Raffel, C.A.: Few-shot parameter-efficient fine-tuning is better and cheaper than in-context learning. *Advances in Neural Information Processing Systems* **35**, 1950–1965 (2022)
49. Liu, X., Ji, K., Fu, Y., Tam, W., Du, Z., Yang, Z., Tang, J.: P-tuning: Prompt tuning can be comparable to fine-tuning across scales and tasks. In: *Proceedings of the 60th Annual Meeting of the Association for Computational Linguistics (Volume 2: Short Papers)*. pp. 61–68 (2022)
50. Liu, Y.Z.K.Z.Z.: Neural prompt search. *arXiv preprint arXiv:2206.04673* (2022)
51. Liu, Z., Lin, Y., Cao, Y., Hu, H., Wei, Y., Zhang, Z., Lin, S., Guo, B.: Swin transformer: Hierarchical vision transformer using shifted windows. In: *Proceedings of the IEEE/CVF international conference on computer vision*. pp. 10012–10022 (2021)
52. Loshchilov, I., Hutter, F.: Sgdr: Stochastic gradient descent with warm restarts. *arXiv preprint arXiv:1608.03983* (2016)

53. Loshchilov, I., Hutter, F.: Decoupled weight decay regularization. arXiv preprint arXiv:1711.05101 (2017)
54. Lyu, H., Sha, N., Qin, S., Yan, M., Xie, Y., Wang, R.: Advances in neural information processing systems. *Advances in neural information processing systems* **32** (2019)
55. Ma, J., Zhao, Z., Yi, X., Chen, J., Hong, L., Chi, E.H.: Modeling task relationships in multi-task learning with multi-gate mixture-of-experts. In: *Proceedings of the 24th ACM SIGKDD international conference on knowledge discovery & data mining*. pp. 1930–1939 (2018)
56. Maji, S., Rahtu, E., Kannala, J., Blaschko, M., Vedaldi, A.: Fine-grained visual classification of aircraft. arXiv preprint arXiv:1306.5151 (2013)
57. Matthey, L., Higgins, I., Hassabis, D., Lerchner, A.: dsprites: Disentanglement testing sprites dataset (2017)
58. Molchanov, D., Ashukha, A., Vetrov, D.: Variational dropout sparsifies deep neural networks. In: *International Conference on Machine Learning*. pp. 2498–2507. PMLR (2017)
59. Nilsback, M.E., Zisserman, A.: Automated flower classification over a large number of classes. In: *2008 Sixth Indian conference on computer vision, graphics & image processing*. pp. 722–729. IEEE (2008)
60. Pan, J., Lin, Z., Zhu, X., Shao, J., Li, H.: St-adapter: Parameter-efficient image-to-video transfer learning. *Advances in Neural Information Processing Systems* **35**, 26462–26477 (2022)
61. Park, J., Lee, J., Sohn, K.: Dual-path adaptation from image to video transformers. In: *Proceedings of the IEEE/CVF Conference on Computer Vision and Pattern Recognition*. pp. 2203–2213 (2023)
62. Parkhi, O.M., Vedaldi, A., Zisserman, A., Jawahar, C.: Cats and dogs. In: *2012 IEEE conference on computer vision and pattern recognition*. pp. 3498–3505. IEEE (2012)
63. Paszke, A., Gross, S., Massa, F., Lerer, A., Bradbury, J., Chanan, G., Killeen, T., Lin, Z., Gimelshein, N., Antiga, L., et al.: Pytorch: An imperative style, high-performance deep learning library. *Advances in neural information processing systems* **32** (2019)
64. Pfeiffer, J., Kamath, A., Rücklé, A., Cho, K., Gurevych, I.: Adapterfusion: Non-destructive task composition for transfer learning. arXiv preprint arXiv:2005.00247 (2020)
65. Pfeiffer, J., Rücklé, A., Poth, C., Kamath, A., Vulić, I., Ruder, S., Cho, K., Gurevych, I.: Adapterhub: A framework for adapting transformers. arXiv preprint arXiv:2007.07779 (2020)
66. Russakovsky, O., Deng, J., Su, H., Krause, J., Satheesh, S., Ma, S., Huang, Z., Karpathy, A., Khosla, A., Bernstein, M., et al.: Imagenet large scale visual recognition challenge. *International journal of computer vision* **115**, 211–252 (2015)
67. Shazeer, N., Mirhoseini, A., Maziarz, K., Davis, A., Le, Q., Hinton, G., Dean, J.: Outrageously large neural networks: The sparsely-gated mixture-of-experts layer. arXiv preprint arXiv:1701.06538 (2017)
68. Sun, C., Shrivastava, A., Singh, S., Gupta, A.: Revisiting unreasonable effectiveness of data in deep learning era. In: *Proceedings of the IEEE international conference on computer vision*. pp. 843–852 (2017)
69. Touvron, H., Martin, L., Stone, K., Albert, P., Almahairi, A., Babaei, Y., Bashlykov, N., Batra, S., Bhargava, P., Bhosale, S., et al.: Llama 2: Open foundation and fine-tuned chat models. arXiv preprint arXiv:2307.09288 (2023)

70. Van Horn, G., Branson, S., Farrell, R., Haber, S., Barry, J., Ipeirotis, P., Perona, P., Belongie, S.: Building a bird recognition app and large scale dataset with citizen scientists: The fine print in fine-grained dataset collection. In: Proceedings of the IEEE conference on computer vision and pattern recognition. pp. 595–604 (2015)
71. Veeling, B.S., Linmans, J., Winkens, J., Cohen, T., Welling, M.: Rotation equivariant cnns for digital pathology. In: Medical Image Computing and Computer Assisted Intervention–MICCAI 2018: 21st International Conference, Granada, Spain, September 16–20, 2018, Proceedings, Part II 11. pp. 210–218. Springer (2018)
72. Wah, C., Branson, S., Welinder, P., Perona, P., Belongie, S.: The caltech-ucsd birds-200-2011 dataset. Tech. Rep. CNS-TR-2011-001, California Institute of Technology (2011)
73. Wang, Y., Agarwal, S., Mukherjee, S., Liu, X., Gao, J., Awadallah, A.H., Gao, J.: Adamix: Mixture-of-adaptations for parameter-efficient model tuning. arXiv preprint arXiv:2210.17451 (2022)
74. Xiao, J., Hays, J., Ehinger, K.A., Oliva, A., Torralba, A.: Sun database: Large-scale scene recognition from abbey to zoo. In: 2010 IEEE computer society conference on computer vision and pattern recognition. pp. 3485–3492. IEEE (2010)
75. Xu, R., Luo, F., Zhang, Z., Tan, C., Chang, B., Huang, S., Huang, F.: Raise a child in large language model: Towards effective and generalizable fine-tuning. arXiv preprint arXiv:2109.05687 (2021)
76. Yu, B.X., Chang, J., Wang, H., Liu, L., Wang, S., Wang, Z., Lin, J., Xie, L., Li, H., Lin, Z., et al.: Visual tuning. arXiv preprint arXiv:2305.06061 (2023)
77. Yun, S., Han, D., Oh, S.J., Chun, S., Choe, J., Yoo, Y.: Cutmix: Regularization strategy to train strong classifiers with localizable features. In: Proceedings of the IEEE/CVF international conference on computer vision. pp. 6023–6032 (2019)
78. Yuval, N.: Reading digits in natural images with unsupervised feature learning. In: Proceedings of the NIPS Workshop on Deep Learning and Unsupervised Feature Learning (2011)
79. Zadouri, T., Üstün, A., Ahmadian, A., Ermiş, B., Locatelli, A., Hooker, S.: Pushing mixture of experts to the limit: Extremely parameter efficient moe for instruction tuning. arXiv preprint arXiv:2309.05444 (2023)
80. Zaken, E.B., Ravfogel, S., Goldberg, Y.: Bitfit: Simple parameter-efficient fine-tuning for transformer-based masked language-models. arXiv preprint arXiv:2106.10199 (2021)
81. Zhai, X., Kolesnikov, A., Houlsby, N., Beyer, L.: Scaling vision transformers. In: Proceedings of the IEEE/CVF Conference on Computer Vision and Pattern Recognition. pp. 12104–12113 (2022)
82. Zhai, X., Puigcerver, J., Kolesnikov, A., Ruysen, P., Riquelme, C., Lucic, M., Djolonga, J., Pinto, A.S., Neumann, M., Dosovitskiy, A., et al.: A large-scale study of representation learning with the visual task adaptation benchmark. arXiv preprint arXiv:1910.04867 (2019)
83. Zhang, H., Cisse, M., Dauphin, Y.N., Lopez-Paz, D.: mixup: Beyond empirical risk minimization. arXiv preprint arXiv:1710.09412 (2017)
84. Zhang, Z., Lin, Y., Liu, Z., Li, P., Sun, M., Zhou, J.: Moefication: Transformer feed-forward layers are mixtures of experts. arXiv preprint arXiv:2110.01786 (2021)
85. Zhang, Z., Zhang, Q., Gao, Z., Zhang, R., Shutova, E., Zhou, S., Zhang, S.: Gradient-based parameter selection for efficient fine-tuning. arXiv preprint arXiv:2312.10136 (2023)
86. Zuo, S., Liu, X., Jiao, J., Kim, Y.J., Hassan, H., Zhang, R., Zhao, T., Gao, J.: Taming sparsely activated transformer with stochastic experts. arXiv preprint arXiv:2110.04260 (2021)